Radiationless transitions to atomic $M_{1,2,3}$ shells: Results of relativistic theory

Mau Hsiung Chen and Bernd Crasemann
Department of Physics and Chemical Physics Institute, University of Oregon, Eugene, Oregon 97403

Hans Mark
National Aeronautics and Space Administration, Washington, D.C. 20546

(Received 4 November 1982)

Radiationless transitions filling vacancies in atomic M_1, M_2, and M_3 subshells have been calculated relativistically with Dirac-Hartree-Slater wave functions for ten elements with atomic numbers $67 \leq Z \leq 95$. Results are compared with those of nonrelativistic calculations and experiment. Relativistic effects are found to be significant. Limitations of an independent-particle model for the calculation of Coster-Kronig rates are noted.

I. INTRODUCTION

It is well known that radiationless transitions to hole states in the K and L shells of medium Z and heavy atoms and to $M_{4,5}$ shells of heavy atoms are considerably affected by relativity.[1-4] No relativistic computations of $M_{1,2,3}$ radiationless transitions have been performed to date, although extensive nonrelativistic calculations of M-shell Auger and Coster-Kronig transitions were carried out by McGuire with approximate Hartree-Slater (AHS) wave functions and transition energies estimated by a semiempirical rule.[5] In the present paper, we report on relativistic calculations of M_1-, M_2-, and M_3-subshell radiationless transition rates for ten elements with $67 \leq Z \leq 95$, based on Dirac-Hartree-Slater (DHS) wave functions and Coster-Kronig energies from relativistic calculations that include relaxation and quantum-electrodynamic (QED) corrections.[6] The purpose of this study is twofold: (i) to establish the effect of relativity on $M_{1,2,3}$-shell radiationless transitions and (ii) to determine the reliability of the independent-particle model in calculations of M-shell Coster-Kronig transitions for medium heavy and heavy elements. This is of particular interest because the independent-particle theory has been found to lead to an overestimation of M-shell super–Coster-Kronig transition rates for light and medium-Z atoms.[7-9]

II. THEORY

The Auger transitions are treated as a two-step process. The Auger decay probabilities are calculated from perturbation theory under the frozen-core approximation. The rates are calculated in j-j coupling. Even though pure j-j coupling is not quite suitable for transitions that involve outer shells, we are interested in *total* transition rates which are independent of the coupling scheme if one neglects the effect of the final-state two-hole splitting.

The total rate for a transition $n_1'\kappa_1' \rightarrow n_1\kappa_1 n_2\kappa_2$ is then

$$T = \tau(2j_1'+1)^{-1} \times \sum_{\substack{J,J' \\ M,M'}} \sum_{\kappa_2'} |\langle j_1' j_2' J' M' | V_{12} | j_1 j_2 J M \rangle|^2 , \tag{1}$$

where

$$\tau = \begin{cases} \frac{1}{2} & \text{if } n_1\kappa_1 = n_2\kappa_2 \\ 1 & \text{otherwise.} \end{cases} \tag{2}$$

The primed quantum numbers j_1' and j_2' pertain to the wave functions of the initial hole and of the hole in the continuum, respectively. The unprimed quantum numbers j_1 and j_2 characterize the final two-hole state. The continuum wave function is normalized to represent one ejected electron per unit time. Atomic units are used throughout.

Equation (1) does not take into account the coupling with open outer shells. This introduces no serious error in the total Auger rate if the coupling does not significantly affect the Auger-electron energy.[10] In all cases treated in the present work, this condition is fulfilled and coupling with open outer shells can be neglected.

From quantum electrodynamics, the electron-electron interaction operator is gauge dependent. In our present relativistic Auger calculations, the two-electron operator is chosen to be the Møller operator, which is based on the Lorentz gauge:

TABLE I. Theoretical M_1-shell Coster-Kronig yields f_{ij}, fluorescence yields ω_1, and level widths $\Gamma(M_1)$ (eV).[a]

Z	f_{12}	f_{13}	f_{14}	f_{15}	ω_1	$\Gamma(M_1)$
67	0.292	0.609	0.082	0.114	9.90(−4)	15.66
70	0.185	0.621	0.080	0.113	1.18(−3)	16.79
74	0.142	0.635	0.086	0.121	1.63(−3)	16.82
78	0.135	0.589	0.087	0.121	2.14(−3)	17.79
80	0.130	0.589	0.088	0.122	2.47(−3)	18.24
85	0.110	0.597	0.091	0.124	3.46(−3)	19.05
88	0.101	0.615	0.096	0.129	4.43(−3)	18.97
90	0.078	0.610	0.096	0.129	4.97(−3)	19.32
92	0.080	0.605	0.097	0.129	5.73(−3)	19.53
95	0.084	0.615	0.100	0.131	6.94(−3)	19.73

[a]Numbers in parentheses signify powers of ten, e.g., $9.90(-4)=9.90\times10^{-4}$.

$$V_{12}=(1-\vec{\alpha}_1\cdot\vec{\alpha}_2)e^{i\omega r_{12}}/r_{12}\ . \quad (3)$$

Here, the $\vec{\alpha}_i$ are Dirac matrices, and ω is the energy of the virtual photon.

In the Coulomb gauge, the two-electron operator is[11]

$$V_{12}=1/r_{12}-(\vec{\alpha}_1\cdot\vec{\alpha}_2)e^{i\omega r_{12}}/r_{12}$$
$$+(\vec{\alpha}_1\cdot\vec{\nabla}_1)(\vec{\alpha}_2\cdot\vec{\nabla}_2)(e^{i\omega r_{12}}-1)/(\omega^2 r_{12})\ . \quad (4)$$

The two-electron matrix elements of Eqs. (3) and (4) are identical whenever the unperturbed electron orbitals satisfy Dirac equations in a local potential.[12] This is the case in the Dirac-Hartree-Slater model used in the present calculations. The matrix elements of Eqs. (3) and (4) are not necessarily identical when evaluated with Dirac-Fock orbitals. It is, however, known that the on-shell matrix elements of Eqs. (3) and (4) give the same results.[13] In first-order perturbation theory, the relativistic Auger rate computed with Dirac-Fock wave functions has been found to be practically gauge invariant.[14] Detailed derivations of the relativistic Auger matrix elements can be found in Ref. 1.

III. NUMERICAL CALCULATIONS

Dirac-Hartree-Slater wave functions corresponding to the initial hole states were used to calculate the Auger radial integrals. The Coster-Kronig transition energies were obtained from relativistic relaxed-orbital calculations that included QED corrections.[15] For Coster-Kronig processes, which are characterized by low transition energies and very energy-sensitive matrix elements, QED corrections are quite important and cannot be neglected; QED effects amount typically to $\sim$10 eV for M_1-MX transitions near $Z\cong92$. The (higher) Auger energies are less critical and were derived by applying the "$Z+1$ rule" to theoretical relativistic neutral-atom

TABLE II. Theoretical M_2- and M_3-shell Coster-Kronig yields f_{ij}, fluorescence yields ω_i, and level widths $\Gamma(M_i)$ (eV).[a]

Z	f_{23}	f_{24}	f_{25}	ω_2	$\Gamma(M_2)$	f_{34}	f_{35}	ω_3	$\Gamma(M_3)$
67	0.099	0.691	0.136	1.72(−3)	9.50	0.144	0.755	1.68(−3)	9.84
70	0.110	0.733	0.128	2.01(−3)	10.28	0.149	0.736	2.15(−3)	9.97
74	0.105	0.707	0.115	2.52(−3)	11.9	0.086	0.784	2.94(−3)	10.56
78	0.107	0.687	0.108	3.18(−3)	13.19	0.101	0.734	4.60(−3)	9.78
80	0.105	0.688	0.107	3.68(−3)	13.63	0.100	0.731	5.27(−3)	10.22
85	0.106	0.674	0.112	5.34(−3)	13.67	0.069	0.742	7.39(−3)	10.96
88	0.102	0.666	0.111	6.38(−3)	14.26	0.072	0.717	9.56(−3)	10.77
90	0.102	0.663	0.114	7.31(−3)	14.51	0.078	0.686	1.16(−2)	10.09
92	0.102	0.659	0.113	8.38(−3)	14.68	0.075	0.683	1.30(−2)	10.37
95	0.106	0.652	0.112	9.82(−3)	15.28	0.067	0.679	1.54(−2)	11.02

[a]Numbers in parentheses signify powers of ten, e.g., $1.72(-3)=1.72\times10^{-3}$.

binding energies.[16] The M_i-subshell fluorescence yields were calculated by combining our relativistic DHS radiationless transition rates with Bhalla's relativistic DHS x-ray rates.[17]

IV. RESULTS AND DISCUSSION

The calculated M_1- and $M_{2,3}$-subshell Coster-Kronig yields, fluorescence yields, and total widths are listed in Tables I and II. Super—Coster-Kronig processes are energetically forbidden for atoms studied in the present work; hence the Coster-Kronig yields f_{ij} are equivalent to the quantities $S_{M_{ij}}$ defined as the average number of M_j holes that arise in the first step of an M_i- hole decay.

The effects of relativity on radiationless transitions can arise from several factors: (i) changes in transition energies; (ii) relativistic orbital effects caused by the inclusion of the mass-velocity correction, the Darwin term, and spin-orbit interaction in the Dirac equations; and (iii) the inclusion of the magnetic interaction and retardation correction in the two-electron operator to account for the electron-photon coupling. The net effect depends on the relative strengths and phases of these factors. Energy effects are obviously very important for Coster-Kronig transitions. Without relativity, some of the M-shell Coster-Kronig transitions would be energetically impossible. In fact, all M_2-M_3X Coster-Kronig transitions, for example, are energetically impossible in the nonrelativistic limit; only spin-orbit splitting makes them possible.

In order to study the relativistic orbital effect and the effects of the magnetic interaction and retardation correction, the radiationless transition rates from the present DHS calculations are compared in Figs. 1—3 with nonrelativistic Hartree-Slater results based on the same relativistic transition energies and with McGuire's values[5,10] from an approximate Hartree-Slater (AHS) model. The relativistic effects are seen to reduce some of the transition rates (e.g., M_2-$N_4N_{6,7}$, M_1-M_3N_4) and to increase some others (e.g., M_2-M_4N_2, M_1-M_4N_1) by amounts ranging from 10% to 50%. The relativisitic orbital effect is the dominant factor. For M_1-$N_{6,7}N_{6,7}$ transitions, the relativistic contraction of the $3s$ and $3p_{1/2}$ orbital wave functions, coupled with the expansion of the $4f$ orbital due to the indirect relativistic effect, drastically reduces the transition rates. The disparity in the effect of the Breit interaction on the various different transitions arises from variations in relative strengths and phases between Coulomb and Breit matrix elements. These amplitudes can add constructively or destructively, producing quite uneven effects on different transitions.

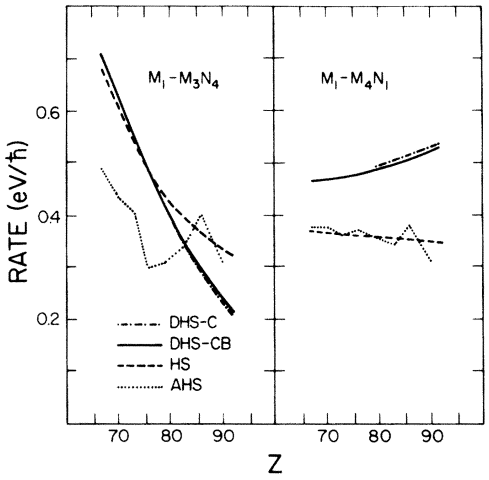

FIG. 1. M_1-M_3N_4 and M_1-M_4N_1 Coster-Kronig transition rates, as functions of atomic number, calculated from relativistic DHS wave functions with the Coulomb interaction only (DHS-C), from DHS wave functions with both the Coulomb and Breit interactions (DHS-CB), from nonrelativistic HS wave functions (HS), and from nonrelativistic approximate HS wave functions (AHS, Refs. 5 and 10).

Some of McGuire's individual transition rates[5] are quite different from the present nonrelativistic Hartree-Slater results (e.g., by a factor of 2 for M_1-$N_{6,7}N_{6,7}$ and by $\sim 40\%$ for M_1-M_3N_4, for $Z < 80$). These discrepancies are partly due to errors in the

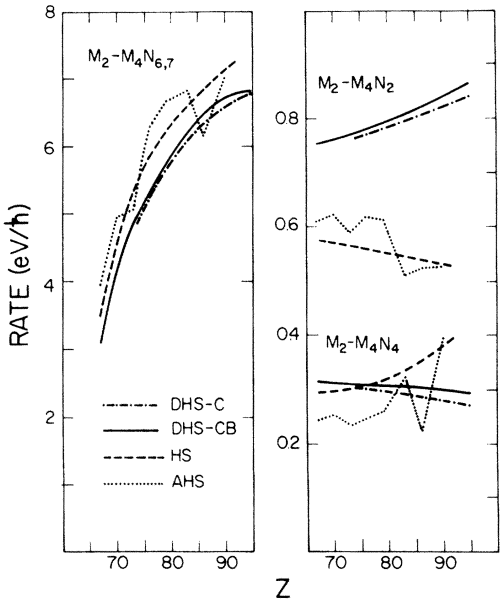

FIG. 2. M_2-$M_4N_{6,7}$, M_2-M_4N_2, and M_2-M_4N_4 Coster-Kronig transition probabilities, as functions of atomic number, calculated from the atomic models identified in the caption of Fig. 1.

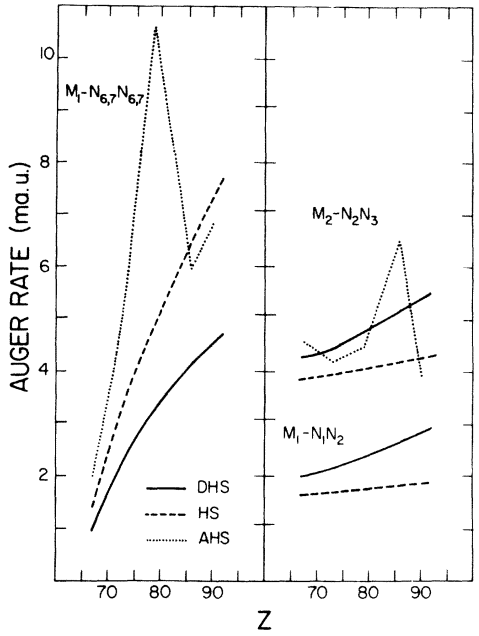

FIG. 3. M_1-$N_{6,7}N_{6,7}$, M_2-N_2N_3, and M_1-N_1N_2 Auger transition rates, as functions of atomic number, computed from relativistic DHS wave functions, nonrelativistic HS wave functions, and nonrelativistic approximate HS wave functions (AHS, Refs. 5 and 10).

transition energies and partly to the straight-line approximation to the Herman-Skillman potential[18] used in Ref. 5. The discrepancies in Coster-Kronig yields and level widths between the present DHS results and those of McGuire[5] are ~(10–25) %.

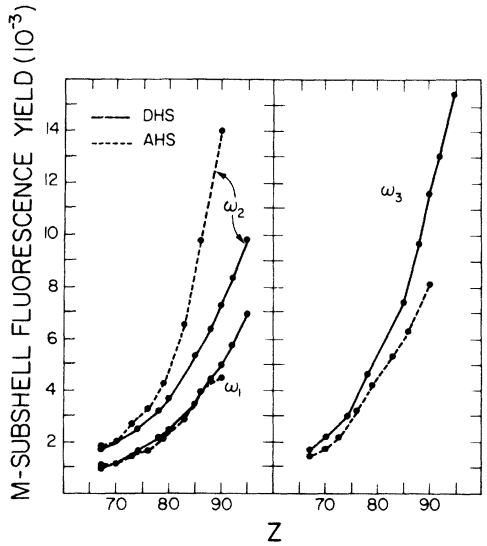

FIG. 4. M_i-subshell fluorescence yields ω_i, as functions of atomic number, computed relativistically from DHS wave functions and nonrelativistically from approximate HS wave functions (AHS, Refs. 5 and 10).

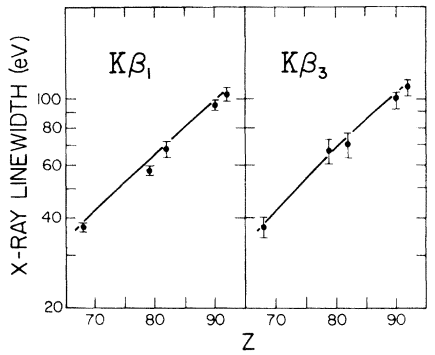

FIG. 5. $K\beta_1$ and $K\beta_3$ x-ray linewidths, as functions of atomic number, from the present relativistic computations with DHS wave functions. Experimental data are from Ref. 19.

The fluorescence yields of the M_i subshells are plotted in Fig. 4 as functions of atomic number. The fluorescence yields ω_i are the ratios of M_i-subshell radiative widths to total (radiative plus radiationless) widths. The radiationless widths were taken from the present work and the radiative widths from Refs. 5 and 17, respectively. It is apparent from Fig. 4 that the M_2 and M_3 fluorescence yields from different calculations differ by as much

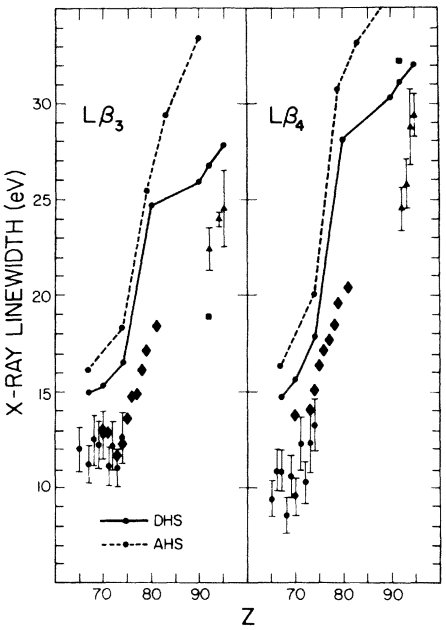

FIG. 6. $L\beta_3$ and $L\beta_4$ x-ray linewidths, as functions of atomic number, computed relativistically from DHS wave functions and nonrelativistically from approximate HS wave functions (AHS, Refs. 5 and 10). Experimental data are from Ref. 20 (dots), Ref. 21 (diamonds), Ref. 22 (triangles), and Ref. 23 (squares).

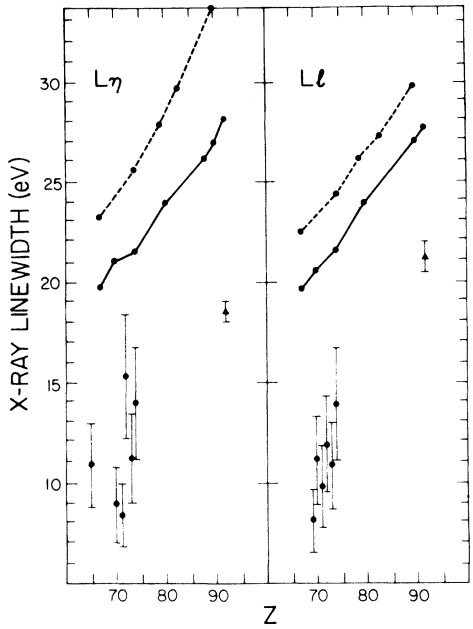

FIG. 7. $L\eta$ and Ll x-ray linewidths, as functions of atomic number. Relativistic calculations from DHS wave functions (solid curves) are compared with nonrelativistic calculations from approximate Hartree-Slater wave functions (AHS, Refs. 5 and 10; dashed curves) and with experimental data: dots, from Ref. 20; triangles, from Ref. 22.

as a factor of 2 for heavy atoms. This variation is mostly due to the discrepancy in radiative rates between nonrelativistic AHS results[5] and those from DHS calculations.[17]

The $K\beta_1$ (K-M_3) and $K\beta_3$ (K-M_2) x-ray linewidths from our DHS calculations are compared with experimental results[19] in Fig. 5. Good agreement between theory and experiment is obtained. In Figs. 6 and 7, the theoretical $L\beta_3$ (L_1-M_3), $L\beta_4$ (L_1-M_2), $L\eta$ (L_2-M_1), and Ll (L_3-M_1) x-ray linewidths are compared with experiment.[20–23] All theories overestimate the linewidths. Our present DHS results show some improvement over the nonrelativistic AHS results.[5] For $L\beta_3$ and $L\beta_4$ x-ray widths, the present DHS results exceed experimental values by $\sim$10—20%, mostly due to the error in L_1-level widths.[24] For $L\eta$ and Ll x-ray lines, the present theory overestimates the widths by $\sim$30—50%, mainly due to the error in M_1 Coster-Kronig transition rates.

V. CONCLUSIONS

The M_1-, M_2-, and M_3-shell radiationless transitions have been calculated relativistically with DHS wave functions, for ten elements with atomic numbers $67 \leq Z \leq 95$. The effect of relativity on individual transition rates is found to be significant (40—50%); it is dominated by the change of wave functions. The present relativistic independent-particle model overestimates $M_{2,3}$ Coster-Kronig rates by $\sim$10—15% and M_1 Coster-Kronig rates by $\sim$30—50% for medium heavy and heavy atoms. To remove this discrepancy, a relativistic many-body calculation is required for heavy atoms.

ACKNOWLEDGMENTS

We thank E. G. Kessler and R. D. Deslattes for communicating results of their group's precision x-ray measurements in advance of publication. This work was supported in part by the U.S. Air Force Office of Scientific Research (Grant No. 79-0026).

[1]M. H. Chen, E. Laiman, B. Crasemann, M. Aoyagi, and H. Mark, Phys. Rev. A 19, 2253 (1979).
[2]M. H. Chen, B. Crasemann, M. Aoyagi, and H. Mark, Phys. Rev. A 20, 385 (1979).
[3]M. H. Chen, B. Crasemann, and H. Mark, Phys. Rev. A 21, 436 (1980); 21, 442 (1980).
[4]M. H. Chen, B. Crasemann, and H. Mark, Phys. Rev. A 21, 449 (1980).
[5]E. J. McGuire, Phys. Rev. A 5, 1043 (1972); 5, 1052 (1972).
[6]M. H. Chen, B. Crasemann, K. N. Huang, M. Aoyagi, and H. Mark, At. Data Nucl. Data Tables 19, 97 (1977).
[7]M. H. Chen, B. Crasemann, M. Aoyagi, and H. Mark, Phys. Rev. A 18, 802 (1978).
[8]M. Ohno and G. Wendin, J. Phys. B 12, 1305 (1979).
[9]D. Hausamann, B. Breuckmann, and W. Mehlhorn, in *Proceedings of International Conference on the Physics of Electronic and Atomic Collisions, 10th, Abstracts of Papers* (Commissariat à l'Energie Atomique, Paris, 1977), Vol. I, p. 208.
[10]E. J. McGuire, in *Atomic Inner-Shell Processes,* edited by B. Crasemann (Academic, New York, 1975), Vol. I, p. 293.
[11]K.-N. Huang, J. Phys. B 11, 787 (1978).
[12]J. B. Mann and W. R. Johnson, Phys. Rev. A 4, 41 (1971).
[13]M. H. Mittleman, Argonne National Laboratory Report No. ANL-80-126 (unpublished), p. 27.
[14]M. H. Chen, in *X-Ray and Atomic Inner-Shell Physics—1982 (International Conference, University of Oregon),* Proceedings of the International Conference on X-Ray and Atomic Inner-Shell Physics, AIP Conf. Proc. No. 94, edited by Bernd Crasemann (AIP, New

York, 1982), p. 331.
[15]M. H. Chen and B. Crasemann (unpublished).
[16]K. N. Huang, M. Aoyagi, M. H. Chen, B. Crasemann, and H. Mark, At. Data Nucl. Data Tables 18, 243 (1976).
[17]C. P. Bhalla, J. Phys. B 3, 916 (1970).
[18]F. Herman and S. Skillman, *Atomic Structure Calculations* (Prentice-Hall, Englewood Cliffs, 1963).
[19]E. G. Kessler (private communication).
[20]S. I. Salem and P. L. Lee, Phys. Rev. A 10, 2033 (1974).
[21]J. N. Cooper, Phys. Rev. 61, 234 (1942); 65, 155 (1944).
[22]J. Merrill and J. W. M. DuMond, Ann. Phys. (N.Y.) 14, 166 (1961).
[23]J. H. Williams, Phys. Rev. 45, 71 (1933); 37, 1431 (1931).
[24]M. H. Chen, B. Crasemann, and H. Mark, Phys. Rev. A 24, 177 (1981).